Irregular many-body dynamics of spinor Bose-Einstein condensates in an optical lattice

Guishu Chong* and F. Borondo†
Departmento de Química C-IX and Instituto Mixto de Ciencias Matemáticas, CSIC-UAM-UC3M-UCM, Universidad Autónoma de Madrid, Cantoblanco-28049, Madrid, Spain
(Received 24 March 2008; published 2 July 2008)

The classical and quantum irregular spin dynamics of atomic spinor Bose-Einstein condensates in an optical lattice, where light-induced and static magnetic dipole-dipole interactions originate the interplay of the condensate at each site, are investigated. Classical-quantum correspondence in the large-spin limit is studied. Quantum chaotic features are studied through analysis of the irregular spectrum and time evolution of the Shannon entropy of wave packets. We show how the optical lattice strength influences the system dynamics, and is responsible for a transition from regular to irregular bahavior.

DOI: 10.1103/PhysRevE.78.016204 PACS number(s): 05.45.Mt, 03.75.Lm, 05.45.Pq, 05.30.Jp

I. INTRODUCTION

Experimental loading of Bose-Einstein condensates (BECs) into optical lattices has opened the possibility for the creation of and research into strongly interacting many-body systems, something traditionally reserved to condensed-matter physics [1,2]. In particular, when quantum many-body correlation effects dominate, making the mean-field approach invalid, the investigations of the quantum features of such dynamical systems constitute a new frontier in BEC studies [3–5]. On the other hand, BEC also offers a new benchmark to explore magnetic properties and spin-dependent dynamics, due to the success in experiment development of trapping and creation of atomic BECs in all-optical potentials [6]. Pu and co-workers [7] argued that BECs confined in optical lattices exhibit ferromagnetic properties, behaving like an array of spin magnets. In their investigations, the static magnetic and/or light-induced dipole-dipole interactions induce coupling between BECs at each site of the lattice, which is different from the exchange interaction of electrons between atoms in the solid state. This new environment has stimulated the present study on the spin dynamics of such systems, in which special attention will be paid to the associated dynamical complexity.

For deep optical lattice potentials and when the spin degrees of freedom are considered, the tight binding method provides a natural connection between the system formed by a BEC in an optical lattice and the lattice spin model [7]. This opens new possible ways to study quantum many-body systems, to perform in various ways quantum-information processing [8], and even to realize special purpose quantum computers, so-called quantum simulators [9]. On the other hand, the integrability of spin lattice systems is also a main research topic [10,11]. Although the phenomenology of BECs in optical lattices is very similar to that of atoms in solid crystals, it has its own peculiarities. For example, due to Bose-enhancement effects, the microcondensations at each site behave like magnets with very large spin quantum numbers; this can be treated to a very good approximation within the classical limit. This provides a good platform to investigate classical-quantum correspondence in chaotic spin dynamics. Additionally, in generic solid materials, the unavoidable effects of impurities can be confused with the eventual chaotic phenomena. BECs in optical lattices offer, however, a cleaner environment. Finally, optical lattices may provide a tunable parameter in an unprecedentedly wide experimental range, which means that the system can be fully and precisely controlled.

In the present work, we investigate classical chaotic spin dynamics and the corresponding irregular spectra at the quantum level for spinor BECs in an optical lattice. The transition to chaos for different energy and system parameters is demonstrated. The dynamical irregularity in the time evolution of the system is also studied, through the evolution of the Shannon entropy of wave packets. As is well known, a linear increase of this entropy with time implies that quantum chaos sets in. The influence of light-induced dipolar interactions on the integrability of the system is also discussed in connection with this process.

The organization of the paper is as follows. In the next section we discuss the model, and the type of calculations we perform in this work. Section III is devoted to the presentation of the corresponding results, which are also thoroughly discussed. Finally, in Sec. IV we summarize the main conclusions that can be derived from our work.

II. SYSTEM AND CALCULATIONS

We consider here BECs loaded into an optical lattice and the static magnetic and/or light-induced dipole-dipole interactions response to the coupling between condensates at each site. Then, under the customary tight binding approximation, the following Hamiltonian can be used as our starting theoretical point [7]:

$$H = \sum_i (\lambda_a' \hat{S}_i^2 - \gamma_B \hat{\vec{S}}_i \cdot \vec{B} - \sum_{j \neq i} J_{ij}^z \hat{S}_i^z \hat{S}_j^z - \sum_{j \neq i} J_{ij} (\hat{S}_i^{(-)} \hat{S}_j^{(+)} + \hat{S}_i^{(+)} \hat{S}_j^{(-)})), \quad (1)$$

where $\hat{\vec{S}}_i$ is the collective spin operator with components $\hat{S}_i^{\{\pm,z\}}$. The first term in the Hamiltonian (1) comes from spin-

*guishu_chong@yahoo.com.cn
†f.borondo@uam.es

dependent interatomic collisions, the second term denotes the coupling of the atoms to an external magnetic field, and the last two terms indicate the coupling caused by the static magnetic field and light-induced dipolar interactions, respectively. The coefficient $2J_{ij}-J_{ij}^z$, which depends only on the light-induced dipole-dipole interaction, is proportional to the strength of the optical lattice field.

Now, we consider the simple case of three sites with periodic boundary conditions. An alternative experimental possibility is that where the BECs are loaded into a triangular Kagomé lattice [12]. When only the nearest neighbor interactions are considered, a triangular three-site model can be decoupled from the whole lattice system [13]. Thus, in Eq. (1) we can restrict the existing indices to $1 \leq i,j \leq 3$. Supposing that the number of BEC atoms at each site, N_i, is the same, the total spin at site i has an identically fixed value expressed as S, which can be a large number because of Bose enhancement. Consequently, the first term in Hamiltonian (1) is a constant, which will be neglected hereafter. Assuming that the external magnetic field is aligned with the z direction, and scaling the Hamiltonian by $\gamma_B B_z$, Eq. (1) can be reduced to a two-parameter Hamiltonian, which reads

$$\mathcal{H} = -\sum_{j=1}^{3} \left(\hat{S}_i^z + \alpha \hat{S}_j^z \hat{S}_{j+1}^z + \frac{1}{2}\alpha(1+\rho)(\hat{S}_j^{(+)}\hat{S}_{j+1}^{(-)} + \hat{S}_j^{(-)}\hat{S}_{j+1}^{(+)}) \right), \tag{2}$$

where $\hat{\vec{S}}_4 = \hat{\vec{S}}_1$, and average values J and J^z have been used in $\rho = (2J - J^z)/J^z$, $\alpha = J^z/(\gamma_B B_z)$ to account for the coefficients J_{ij} and J_{ij}^z, respectively. Obviously, for a given external magnetic field, these two parameters α, ρ, characterizing the static magnetic and light-induced dipole-dipole interactions, respectively, can be varied by modulating the optical lattice setup. For simplicity, we fix the parameter $\alpha = 1$ throughout the paper, and change the value of ρ to explore the effects caused by the light-induced interaction.

III. RESULTS AND DISCUSSION

In the classical limit, $\hat{\vec{S}}_j$ is a three-component vector obeying the equations of motion $d\hat{\vec{S}}_j/dt = \{\hat{\vec{S}}_j, \mathcal{H}\} = \hat{\vec{S}}_j \times (-\delta\mathcal{H}/\delta\hat{\vec{S}}_j)$, where $\{\cdots\}$ indicates a classical Poisson bracket. Here, we suppose that the spin magnitude of each microcondensation is conserved, due to the fact that the number of condensed atoms in each site is fixed. It is easy to verify that, in addition to the energy being a conserved quantity, the three components of $\vec{T} = \Sigma_{j=1}^3 \vec{S}_j$ are also constants of the motion for the isotropic case $\rho = 0$. Furthermore, only $T^z = \Sigma_{j=1}^3 S_j^z$ is an invariant constant for the anisotropic case $\rho \neq 0$. So we have effectively two- and four-dimensional phase space for the isotropic limit and anisotropic case, respectively, showing that it is the parameter ρ that makes the system change from integrability to chaoticity. Accordingly, the system Hamiltonian can be split into two parts $\mathcal{H} = \mathcal{H}_0 + \mathcal{H}'$, where $\mathcal{H}_0$ corresponds to the integrable isotropic case and $\mathcal{H}'$ is the perturbation, which is proportional to the light-induced interaction parameter ρ. We now define each spin with the aid of polar and azimuthal angles, so that $\hat{\vec{S}}_j = S(\sin\theta_j \cos\phi_j,\ \sin\theta_j \sin\phi_j,\ \cos\theta_j)$. Now, taking into account the condition $\cos\theta_1 + \cos\theta_2 + \cos\theta_3 = T^z$, it is easy to verify that the energy of the system is associated with four independent initial polar and azimuthal angles.

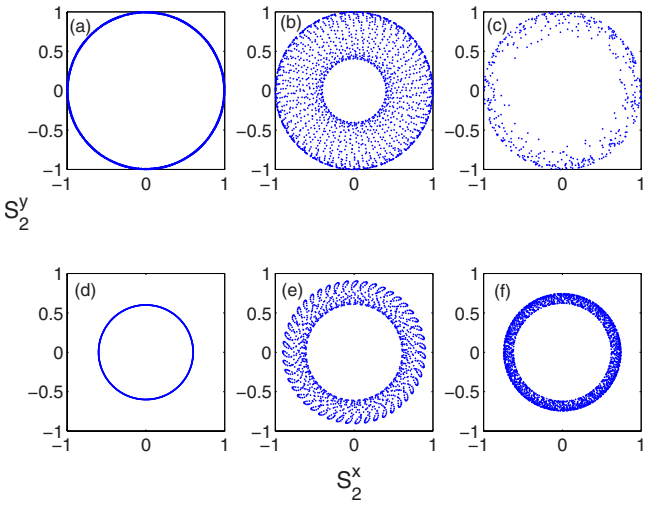

FIG. 1. (Color online) Poincaré surfaces of section in the plane (S_2^x, S_2^y). Initial conditions $\phi_1(0)=0$, $\theta_2(0)=\pi/2$, $\phi_3(0)=0$ are fixed. In the top row, the interaction parameter $\rho=0.5$ and (a) $\theta_1(0)=0.5$, $\phi_2(0)=0$, and thus $E=-2.9426$; (b) $\theta_1(0)=1$, $\phi_2(0)=2\pi/3$, $E=0.100\,34$; (c) $\theta_1(0)=0.5$, $\phi_2(0)=\pi$, $E=1.273\,56$. In the bottom row, $E=0.4$, $\phi_2(0)=2\pi/3$, and (d) $\theta_1(0)=0.08$, $\rho=0.001$; (e) $\theta_1(0)=0.14$, $\rho=0.08$; (f) $\theta_1(0)=0.331$, $\rho=0.5$.

In the classical limit, the corresponding dynamics can be analyzed with the aid of Poincaré surfaces of section. We will take the spin magnitude $S=1$, without loss of generality. In our case the surfaces of section will be plotted in the plane of (S_2^x, S_2^y) and represent the points obtained when the orbits $\vec{S}_1$ positively cross $dS_1^z/dt = 0$. Some results are shown in Fig. 1. In the top row, the plots corresponding to different initial conditions, such that $E=-2.9426$ (a), $0.100\,34$ (b), and $1.273\,56$ (c), are shown. As can be seen, when the energy of the system increases, an increasing number of regular orbits in phase space are destroyed, and chaos emerges, being dominant at the higher energy considered. In the bottom row, we present results corresponding to a fixed value of the system energy, taken equal to $E=0.4$. Different optically induced dipole-dipole interactions corresponding to $\rho = 0.001, 0.08, 0.5$ have been used [Figs. 1(d)–1(f)]. The results show that the system undergoes a transition from regular to chaotic dynamics as the parameter ρ increases.

Let us proceed now to describe our quantum study, which is twofold. First, we have investigated the distributions of the quantum energy levels. Second, we have also considered the issue of the time evolution of wave packets, by using a dynamical entropy to gauge the associated phenomena [14–16]. Due to the C_{3v} symmetry of the system, it is convenient to choose the following basis states [10] for our study:

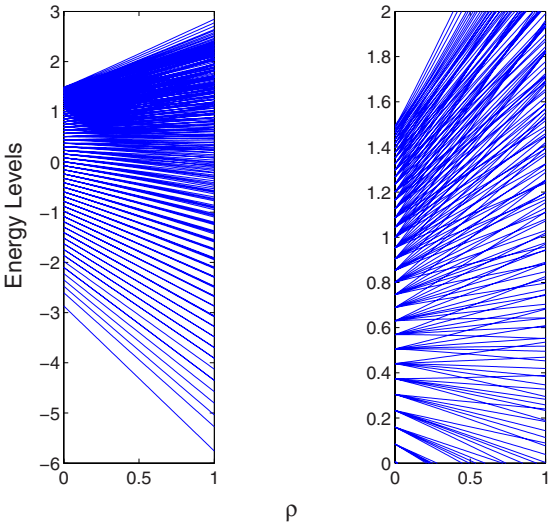

FIG. 2. (Color online) Energy spectrum of the system for $S=21.5$. In the right panel an enlargement is presented. The irregular distribution in the high-energy regime, where the classical counterpart shows a chaotic dynamics, is apparent.

$$\Phi_{\pm}^{K}=\frac{1}{\sqrt{2}}\Bigg(\frac{1}{\sqrt{3}}[(|S,m_a\rangle_1\otimes|S,m_b\rangle_2\otimes|S,m_c\rangle_3+e^{-iK}|S,m_b\rangle_1\otimes|S,m_c\rangle_2\otimes|S,m_a\rangle_3+e^{-2iK}|S,m_c\rangle_1\otimes|S,m_a\rangle_2\otimes|S,m_b\rangle_3)\pm(\text{cycle in } m_a\to m_c\to m_b)]\Bigg), \tag{3}$$

with $m_{a,b,c}=(-S,-S+1,\ldots,S-1,S)$. Here, the wave number K $(0,2\pi/3,4\pi/3)$, parity $(+1,-1)$, and magnetization $T^z=m_a+m_b+m_c$ are the quantum numbers that characterize the basis vectors. Using the relationships ${}_i\langle S,m'|S_i^z|S,m\rangle_i=m\delta_{m'm}$ and ${}_i\langle S,m'|S_i^{\pm}|S,m\rangle_i=[(S\mp m)(S\pm m+1)]^{1/2}\delta_{m',m\pm1}$, which are well known in spin physics, the matrix for the Hamilton can be constructed. The actual values of $K=0$ and $T^z=1/2$ for the quantum numbers and $+1$ for the parity were chosen. The corresponding energies for $S=21.5$, scaled using $S(S+1)$, are shown in Fig. 2 as a function of the light-induced dipole-dipole interaction parameter ρ.

Let us remark that the results we have presented correspond to a (relatively) large value of S, and thus the validity of the semiclassical limit can be assumed. In this situation, there are qualitatively different structures appearing in different energy intervals, depending on whether the classical counterparts have predominantly regular or chaotic orbits in that interval. As demonstrated in Fig. 2, in the high-energy region, energy levels appear irregularly distributed, while well-separated clustered level structures are typical in the low-energy region. The existence of level repulsions, characteristic of irregular spectra, can be clearly seen in the right part of the figure, where an enlarged portion of the whole set of data is shown. Starting at the integrable limit $\rho\to0$, the levels start from a series of degenerate energies, and then they split. As these separations broaden as ρ increases, the levels reach a point at which they start to interact significantly and then strongly mix. In this regime, an irregular spectrum for highly excited states emerges. In other words, by modulating the optical lattice strength, the highly excited states of system undergo a transition from regular to chaotic. From another point of view, this kind of transition from regular to chaotic in the quantum case for large values of the spin quantum numbers (semiclassical limit) is not unexpected when the classical corresponding behavior is considered. The irregular distribution and level clustering is nothing but the manifestation of chaoticity in the most classical orbits present in Figs. 1(b), 1(c), 1(e), and 1(f), and the regular behavior of those orbits in Figs. 1(a) and 1(d). The origin of chaos in this system in the highly excited large-spin states is related to the very high density of levels existing in this portion of the spectrum. In it, the density of states increases extremely fast (typically exponentially) with both spin magnitude and energy. As a consequence, the spacing between these large-spin levels is exponentially small and any "residual" interaction mediated by the value of the parameter ρ greatly affects the integrability of the system. In this way, a large number of levels mix in the integrable limit.

Due to the extremely high density of energy levels, it is often impossible to resolve individual large-spin levels. Therefore, apart from investigations on quantum chaos that are carried out from the stationary dynamical point of view, it is also necessary to study the time-dependent properties of the system, in order to explore the signatures of quantum chaos in it. In order to investigate chaotic features in highly excited states, entropy is a very appropriate quantity to characterize the dynamical properties of this system [14–16]. Here, we choose to use the eigenstates $|j\rangle$ of the integrable part in the full Hamiltonian $\mathcal{H}_0$ as the basis set in which to span our Hilbert space. Once the optical lattice is switched on, the perturbation $\mathcal{H}'$ sets in. If we now expand the system state $|\psi(t)\rangle$ as a superposition of the above defined eigenstates, the corresponding Shannon entropy can be defined as $S(t)=-\Sigma_j|\psi_j(t)|^2\ln|\psi_j(t)|^2$, with $\psi_j(t)=\langle j|\psi(t)\rangle$ being the projections of $|\psi(t)\rangle$ onto the basis elements $|j\rangle$. For any given initial wave packet $\psi(0)$, the wave function evolves according to the Hamiltonian as $\psi(t)=e^{-i\mathcal{H}t/\hbar}\psi(0)$. Projecting it over the basis elements $|j\rangle$, the Shannon entropy is then easily determined computationally. Obviously, the Shannon entropy allows the estimation of the effective number $N_{\text{eff}}\approx e^{S(t)}$ of states in the integrable case that are involved in the dynamics due to the optically induced light-induced interaction.

Let us now focus our attention on the evolution of the entropy with time, for different excited states. Let us note the importance of this magnitude as a signature to characterize quantum chaos. In our case, we will take the basis set of initial states, $\{|j\rangle\}$, formed by states numbers 5, 70, 135, 200, 265, and 330 with spin magnitude $S=25.5$, and evolve these initial wave packets with $\rho=0.5$. The results for the corresponding entropies are shown in Fig. 3. For low-energy states (e.g., $n=5,70$), there are obvious oscillations in the evolution of the entropy with time, which are just manifestations of the quantum fluctuations. However, for the highly excited states ($n=135,200,265,330$), the entropy increases, tending to a saturation value. The enhancement of the entropy is due to the spread of the wave packets on the basis of integrable case, and the saturation is caused by the finiteness of the Hilbert space. In particular, we find that for

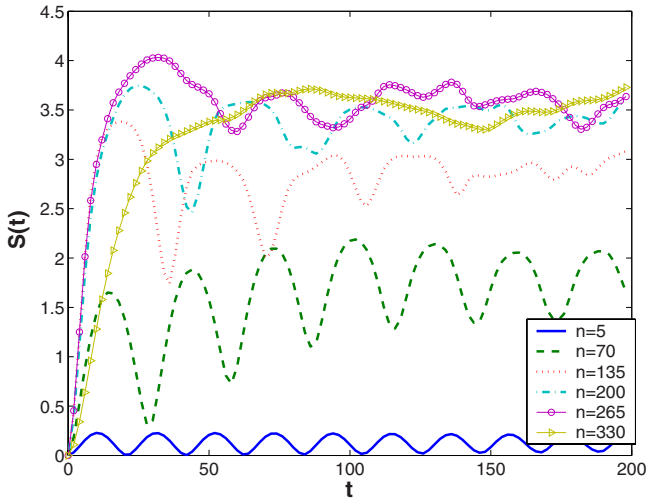

FIG. 3. (Color online) Time evolution of the entropy for different initial excited eigenstates (of the integrable case) for a system with a (large) value of the spin $S=25.5$ and $\rho=0.5$.

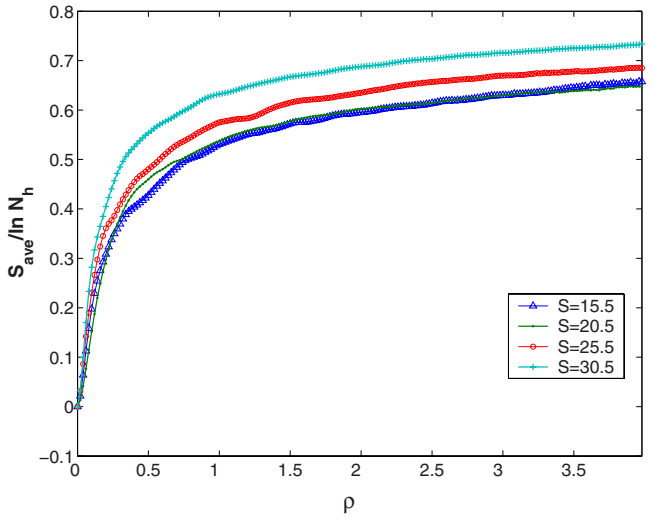

FIG. 4. (Color online) Normalized average entropy as a function of the optically induced interaction parameter ρ for different spin magnitudes given by $S=15.5+5n$ with $n=0$, 1, 2, and 3.

$n=135,200,265$, the entropy increases with time linearly until it gets to a saturation value, this being an important signature of quantum chaos [14–16]. This kind of linear tendency implies that there is an exponential increase in the effective number of principal components present in the wave packet, and this state is populated ergodically in the basis. In other words, this highly excited large-spin state appears as a "chaotic" superposition of the basis states.

In order to see the influence of the optical lattice strength on the transition from regular to chaotic behavior in our system, we have calculated the average entropy versus ρ. Some results for different values of the spin magnitude are shown in Fig. 4. Here, we have chosen the spin magnitude at each site to be $S=15.5$, 20.5, 25.5, and 30.5, which give different dimensions N_h for the Hilbert space. The initial states are selected as the eigenstates of $\mathcal{H}_0$ corresponding to the center of the spectrum, where the many-body density of states is large, and thus a small interaction drives the system into the chaotic regime. After averaging the entropy along the total propagated time, we plot the averaged entropy, divided by N_h, as a function of the parameter ρ in Fig. 4. One can see that the scaled entropy is a quantity that is very sensitive to transition from the regular to the chaotic regime. As shown in the figure, the average entropy changes from a very low value to a high plateau, as the optical strength parameter increases. Accordingly, for the highly excited large-spin states of the system, quantum chaos sets in when the optical parameter is modulated above a certain value.

IV. SUMMARY

Summarizing, in this paper we have studied the classical and quantum dynamics of a Bose-Einstein condensate in a three-site optical lattice, taking the long-range magnetic and optically induced dipole-dipole interactions into account. In the classical case, the existing chaotic dynamical structures are revealed with the aid of Poincaré surfaces of section. The quantum spectrum has also been presented and discussed, showing clear evidence of irregularity in the high-energy regime. As a complement, we have also investigated the time evolution of the Shannon entropy of the system, finding that the highly excited large-spin states can be viewed as a "chaotic" superposition of the Hilbert basis. The influence of the optical induced parameter on the onset of chaos has also been demonstrated by performing an analysis of the averaged properties of the entropy.

ACKNOWLEDGMENTS

The authors thank Dr. J. Brand for useful discussions on the dipole interaction in BECs. Support from MEC, Spain (under Contract Nos. MTM2006-15533, SAB2005-0019, and i-MATH CSD2006-32), and Comunidad de Madrid, Spain (Contract No. SIMUMAT S-0505/ESP-0158) is gratefully acknowledged.

[1] M. Greiner, O. Mandel, T. Esslinger, T. W. Hänsch, and I. Bloch, Nature (London) **415**, 39 (2002).
[2] T. Stöferle, H. Moritz, C. Schori, M. Köhl, and T. Esslinger, Phys. Rev. Lett. **92**, 130403 (2004).
[3] A. Sörensen, L.-M. Duan, J. I. Cirac, and P. Zoller, Nature (London) **409**, 63 (2001).
[4] G. P. Berman, F. Borgonovi, F. M. Izrailev, and A. Smerzi, Phys. Rev. Lett. **92**, 030404 (2004).
[5] A. Argüelles and L. Santos, Phys. Rev. A **75**, 053613 (2007).
[6] M. D. Barrett, J. A. Sauer, and M. S. Chapman, Phys. Rev.

Lett. **87**, 010404 (2001).
[7] C. K. Law, H. Pu, and N. P. Bigelow, Phys. Rev. Lett. **81**, 5257 (1998); H. Pu, W. Zhang, and P. Meystre, *ibid.* **87**, 140405 (2001); **89**, 090401 (2002); W. Zhang, H. Pu, C. Search, and P. Meystre, *ibid.* **88**, 060401 (2002).
[8] O. Mandel, M. Greiner, A. Widera, T. Rom, T. W. Hänsch, and I. Bloch, Nature (London) **425**, 937 (2003).
[9] J. I. Cirac and P. Zoller, Phys. Today **57** (3), 38 (2004).
[10] K. Nakamura, *Quantum Chaos: A New Paradigm of Nonlinear Dynamics* (Cambridge University Press, Cambridge, UK, 1993).
[11] G. Müller, Phys. Rev. A **34**, 3345 (1986).
[12] B. Damski, H. Fehrmann, H.-U. Everts, M. Baranov, L. Santos, and M. Lewenstein, Phys. Rev. A **72**, 053612 (2005).
[13] C. Lee, T. J. Alexander, and Y. S. Kivshar, Phys. Rev. Lett. **97**, 180408 (2006).
[14] V. V. Flambaum and F. M. Izrailev, Phys. Rev. E **56**, 5144 (1997); **64**, 036220 (2001).
[15] X. Wang, S. Ghose, B. C. Sanders, and B. Hu, Phys. Rev. E **70**, 016217 (2004).
[16] C. Mejía-Monasterio, G. Benenti, G. G. Carlo, and G. Casati, Phys. Rev. A **71**, 062324 (2005).